Identification of a Polymorphic Mucin-like Gene Expressed in the Midgut of the Mosquito, *Aedes aegypti*, Using an Integrated Bulked Segregant and Differential Display Analysis

Isabelle Morlais and David W. Severson

Center for Tropical Disease Research and Training, Department of Biological Sciences, University of Notre Dame, Notre Dame, Indiana 46556

Manuscript received October 2, 2000
Accepted for publication April 11, 2001

ABSTRACT

The identification of putative differentially expressed genes within genome regions containing QTL determining susceptibility of the mosquito, *Aedes aegypti*, to the malarial parasite, *Plasmodium gallinaceum*, was investigated using an integrated, targeted approach based on bulked segregant and differential display analysis. A mosquito F_2 population was obtained from pairwise matings between the parasite-susceptible RED strain and the resistant MOYO-R substrain. DNA from female carcasses was used to genotype individuals at RFLP markers of known chromosomal position around the major QTL (*pgs 1*). Midguts, dissected 48 hr after an infected blood meal, were used to prepare two RNA bulks, each representing one of the parental genotypes at the QTL interval. The RNA bulks were compared by differential display PCR. A mucin-like protein gene (*AeIMUC1*) was isolated and characterized. The gene maps within the *pgs 1* QTL interval and is expressed in the adult female midgut. *AeIMUC1* RNA abundance decreased with time after blood meal ingestion. No differential expression was observed between the two mosquito strains but three different alleles with inter- and intrastrain allelic polymorphisms including indels and SNPs were characterized. The *AeIMUC1* gene chromosome location and allelic polymorphisms raise the possibility that the protein might be involved in parasite-mosquito interactions.

MALARIA occurs in more than 90 countries and the World Health Organization estimates that the disease affects 300–500 million people and kills over 1 million young children each year, mostly in sub-Saharan Africa. Transmission of the Plasmodium parasite to a human host is totally dependent upon the availability of a competent mosquito vector. Strategies for malaria control are numerous, largely based on preventive and/or therapeutic drug administration and on vector control measures such as insecticide applications. However, the increase of both parasite drug resistance and mosquito insecticide resistance has reduced control efficiency. New malaria disease control strategies are needed. Vector-based control could be achieved by genetic approaches if, for example, transmission-blocking proteins were identified (Crampton *et al.* 1994; Collins and Paskewitz 1995).

The mosquito vector acquires Plasmodium parasites while blood-feeding on an infected vertebrate host. In the mosquito midgut lumen, male and female gametes escape from the red blood cells, undergo fertilization and the resulting zygotes evolve into motile ookinetes. The ookinetes must then pass through the peritrophic matrix, penetrate the midgut epithelial cells, and lodge on the basal lamina where they transform into oocysts. Maturation of the oocysts leads to sporozoite release into the hemocoel. The sporozoites migrate to the salivary glands and are inoculated into a new vertebrate host when the mosquito feeds.

Plasmodium development in the mosquito midgut progresses in concert with blood meal digestion and therefore the parasite has to confront both physical and biochemical barriers. The peritrophic matrix (PM) is an extracellular layer that forms around the food bolus in the guts of most arthropods (Peters 1992; Tellam 1996). Although its function is not clearly defined, it likely protects the gut epithelium from damage by food particles, facilitates digestion, and also acts as a protective barrier against pathogens (Peters 1992; Tellam 1996). The PM is composed of chitins, proteins, and proteoglycans integrated in a sheet-like structure that Plasmodium ookinetes must cross to reach the midgut epithelium. The mosquito midgut is a monolayer of epithelial cells standing on a continuous basal lamina. The apical side of the epithelial cells is folded into microvilli and covered with glycocalyx (Lehane 1996). Interactions between the parasite and the mosquito midgut determine the developmental fate of ookinetes and subsequently the successful transmission of malaria (Shahabuddin 1998). Understanding the genetic mechanisms involved in susceptibility and refractoriness of mosquito species to Plasmodium will help to identify candidate genes suitable for genetic manipulation of mosquito vector competence.

Corresponding author: David W. Severson, Department of Biological Sciences, University of Notre Dame, Notre Dame, IN 46556.
E-mail: david.w.severson.1@nd.edu

Aedes aegypti and *Plasmodium gallinaceum* constitute a vector-parasite model of choice for studies investigating the genetic basis for vector competence for human malaria (Kilama and Craig 1969; Thathy *et al.* 1994). A linkage map based on restriction fragment length polymorphisms (RFLP) has been developed for *A. aegypti* (Severson *et al.* 1993) and these markers have been used to identify quantitative trait loci (QTL) that determine *P. gallinaceum* susceptibility (*pgs*). Two QTL affecting *pgs* have been identified: a major QTL, *pgs 1*, located on chromosome 2 and a minor QTL, *pgs 2*, on chromosome 3 (Severson *et al.* 1995). Targeting the identification of differentially transcribed sequences within the genome regions carrying QTL could provide an effective approach for isolating genes associated with vector competence.

Bulked segregant analysis (BSA) provides a method to focus on regions containing QTL of interest. BSA involves screening for differences between pooled DNA samples (Michelmore *et al.* 1991). Individuals are selected from a population segregating for a trait of interest and bulked pools are prepared with DNA from individuals containing identical parental genotypes across the target region. The resultant bulks will reflect DNA polymorphisms linked to the target region. BSA has already been used successfully to identify specific random markers linked with traits of interest (Giovannoni *et al.* 1991; Michelmore *et al.* 1991; Severson *et al.* 1999).

Differential display PCR (DD-PCR) of RNA has been described as a powerful technique to identify differentially expressed genes (Liang and Pardee 1992). This technique is based on the random amplification of fragments from first-strand cDNA using a combination of an anchored oligo(dT) primer and a random oligonucleotide primer. The method has been used successfully to identify differentially expressed genes (Dimopoulos *et al.* 1996; Kang *et al.* 1996; Schroeder *et al.* 1999). Nevertheless, drawbacks such as the large number of false positives generated are often reported and different methods have been proposed to facilitate the identification of putative genes (Liang *et al.* 1993; Luce and Burrows 1998; Frost and Guggenheim 1999; Kohroki *et al.* 1999).

In this study, we report an integrated, targeted approach to identifying putative differentially expressed genes within genome regions containing QTL. We initially used the bulked segregant approach to genotype *A. aegypti* F_1 intercross progeny at RFLP marker loci across the *pgs 1* QTL. These progeny had been dissected to remove their midguts ~48 hr following a *P. gallinaceum*-infected blood meal, and the midguts were stored at −80°. To target differential RNA expression, we pooled total RNA extracted from dissected mosquito midguts, with individual midguts selected on the basis of RFLP marker genotypes as determined from the mosquito carcass following midgut removal (*e.g.*, susceptible *vs.* refractory genotypes at the QTL). We then used RT-PCR and the differential display technique to identify several putative differentially expressed cDNA sequences. We have used these procedures to identify and characterize a mucin-like gene. The gene has been recently cloned independently by others and has been named *AeIMUC1* for *A. aegypti* intestinal mucin (Rayms-Keller *et al.* 2000). We have adopted its prior name. Here we report that the gene maps within the *pgs 1* QTL interval and is expressed only in the *A. aegypti* adult female midgut. Interestingly, this gene does not show differential expression between the susceptible and refractory mosquito strains, but does reflect several strain-specific single nucleotide substitutions and indels that result in putative polypeptide product polymorphisms.

MATERIALS AND METHODS

Mosquitoes and parasites: Mosquito strains were reared in an environmental chamber at 26°, 84% relative humidity, under a 16-hr light/8-hr dark cycle with a 1-hr crepuscular period at the beginning and the end of each light cycle. Adults were maintained on a 5% sucrose solution. Female mosquitoes were blood-fed on anesthetized rats or on infective white Leghorn chicks.

The *P. gallinaceum* strain is routinely maintained in the laboratory by natural sporozoite transmission between the *A. aegypti* RED strain and chicks. One-week-old birds are infected by exposure to infected mosquitoes. The parasitemia is monitored daily on thin Giemsa-stained blood smears from 1 week after the infection until a gametocytemia range of 1–3% is reached.

Genetic crosses were performed to obtain F_1 intercross progeny between the *P. gallinaceum*-susceptible *A. aegypti* RED strain and the *P. gallinaceum*-resistant *A. aegypti* MOYO-R substrain. MOYO-R substrain derives from the Moyo-In-Dry strain. Selection of the substrain and relative susceptibilities of the MOYO-R substrain and the RED strain are described by Thathy *et al.* (1994).

F_2 female mosquitoes, 5–10 days old, were infected by feeding on infective chicks for ~15 min. Completely engorged females were then separated and maintained in groups of 15 individuals until dissection. For each dissection experiment, a group of engorged females was retained for midgut dissections 7 days after blood-feeding, to check both prevalence and intensities of infection as indicated by the number of developing oocysts. Some females were also routinely fed on uninfected chicks as parasite negative controls.

F_1 intercross females used for the DD-PCR analysis were dissected 48 hr after the infective blood meal. We chose 48 hr after feeding because by this time, in susceptible individuals, the ookinetes should have crossed the midgut epithelium and should actively be developing into oocysts. Midguts were carefully removed and individually homogenized in 20 μl of Tri Reagent (Molecular Research Center, Inc., Cincinnati, OH) and 0.2 μl of Polyacryl Carrier (Molecular Research Center, Inc.). Midgut homogenates were stored at −80° until RNA extractions. The remaining mosquito carcass was homogenized in 200 μl of DNA extraction buffer using a Tissue Tearor (Biospec, Bartlesville, OK) and DNA extractions were performed as previously described (Severson 1997).

With mosquitoes used for semiquantitative RT-PCR (see below), midguts were dissected at several hours postinfection (hpi), *i.e.*, 24, 48, and 72 hpi and 7 days postinfection, and

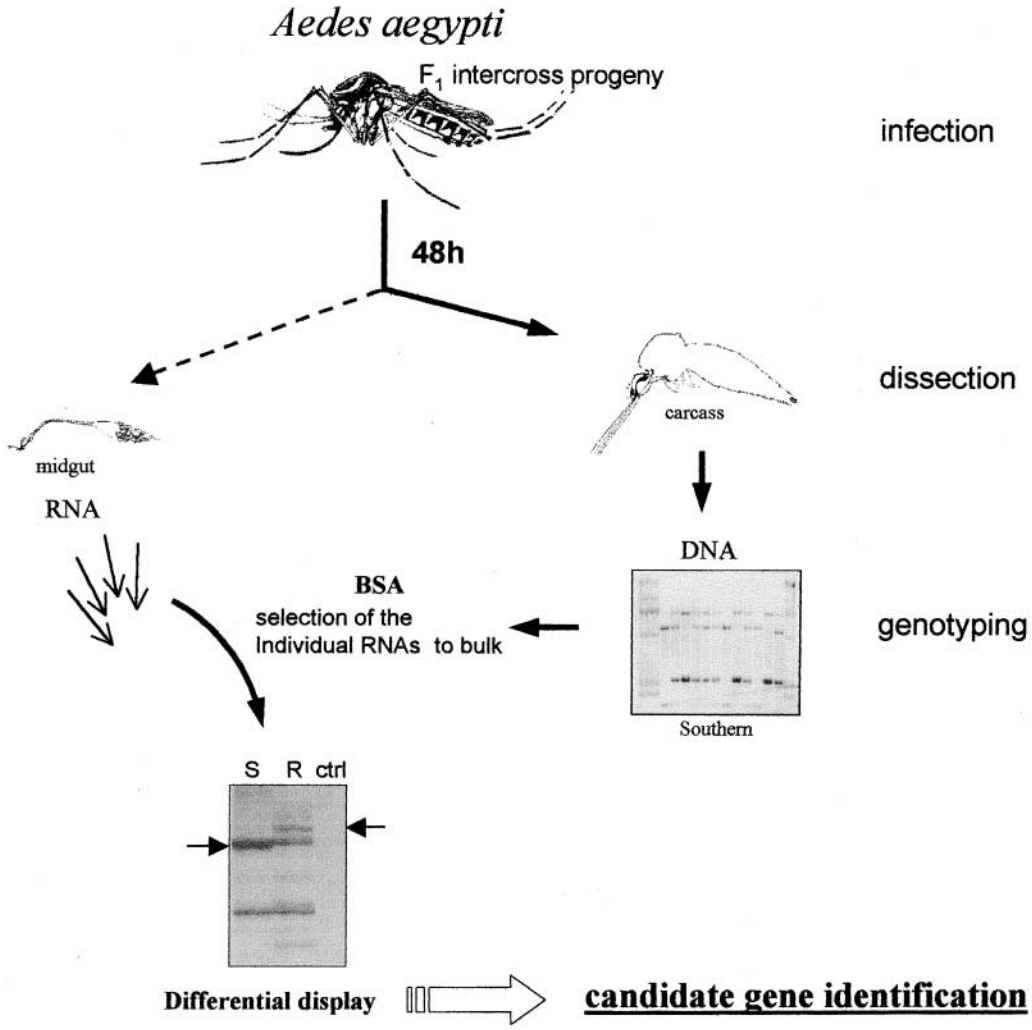

FIGURE 1.—Schematic description of the BSA-DD approach. Genetic crosses were performed between the *P. gallinaceum*-susceptible *A. aegypti* RED strain and the *P. gallinaceum*-resistant *A. aegypti* MOYO-R substrain and the F_1 intercross progeny were fed on infective chicks. Females were dissected 48 hr after the blood meal. Midguts were removed and stored separately until the RNA extraction. Genotyping was performed at RFLP marker loci across the *pgs 1* QTL on DNA extracted from the mosquito carcass. Two RNA pools were prepared with individual midguts from female mosquitoes that showed susceptible *vs.* refractory genotypes at the QTL interval. The two RNA bulks were compared by DD-PCR and the putative differentially expressed cDNAs were identified.

RNA extractions were performed on bulked samples of 15 midguts.

BSA-DD assay by selective genotyping using RFLP markers: For BSA, DNA extraction from individual F_1 intercross females ($n = 155$), digestion by *Eco*RI, Southern blotting, and hybridizations were performed as previously described (SEVERSON 1997). Southern blots were exposed to phosphorimaging screens (Molecular Dynamics, Sunnyvale, CA) and scanned using a Storm 840 phosphorimaging system (Molecular Dynamics).

All individuals were genotyped at the LF338, LF181, LF282, and LF272 loci on chromosome 2. The RFLP probes were chosen on the basis of their known chromosomal positions around the major QTL (*pgs 1*) determining *P. gallinaceum* susceptibility in *A. aegypti* (SEVERSON *et al.* 1995). The RFLP genotypes were then used for identifying individuals suitable for preparing two RNA bulks for differential display analysis (Figure 1). Procedures for the selective genotyping are described elsewhere (SEVERSON *et al.* 1999).

RNA extraction and differential display PCR: Midgut homogenates preserved in Tri Reagent were bulked as described above and total RNA was isolated according to the manufacturer's instructions.

DD-PCR was performed using the Delta differential display kit (Clontech, Palo Alto, CA). Two to five hundred nanograms of total RNA were reverse transcribed using Superscript II RNaseH$^-$ reverse transcriptase (GIBCO-BRL, Gaithersburg, MD) and an anchored oligo(dT) primer. The resulting single-stranded cDNA was amplified by PCR with 1× Advantage KlenTaq polymerase mix (Clontech) using a pairwise combination of arbitrary primers and oligo(dT) primers in the presence of [α-^{33}P]dATP (3000 Ci/mmol; ICN, Costa Mesa, CA). Long-distance PCR was performed using a thermocycler (Hybaid) according to the DD-PCR kit recommendations except that the cycle number was increased: 1 cycle of 94° for 5 min, 40° for 5 min, and 68° for 5 min; 5 cycles of 94° for 2 min, 40° for 5 min, and 68° for 5 min; and 30 cycles of 94° for 1 min, 60° for 1 min, and 68° for 2 min followed by a final extension at 68° for 10 min. The labeled amplified fragments were separated on 5% denaturing polyacrylamide gels at 50 W for 4 hr. Gels were dried and exposed to X-ray film for 24 hr. The film and original gel were aligned using Identi-kit stickers (Sigma, St. Louis) and bands of interest, *e.g.*, differentially displayed, were then excised using a razorblade. The DNA was eluted from the gel by boiling in pyrocarbonic acid diethyl ester-treated water for 5 min. An aliquot of 7 μl of the eluted cDNA was reamplified by PCR with the same primer set used to generate the original band. The reamplified PCR product was separated on a 1.2% LMT agarose gel, excised using a razorblade and the DNA was purified using Ultrafree-DA (Millipore, Bedford, MA).

cDNA cloning and sequencing: The gel-purified cDNA was ligated to pCR-2.1 vector (TOPO TA cloning kit, Invitrogen, San Diego) and the recombinant plasmids were transformed

into competent *Escherichia coli* TOP10 cells (Invitrogen). Recombinant plasmids were purified from overnight cultures using the alkaline lysis technique (Sambrook *et al.* 1989). Plasmid templates were subjected to cycle sequencing using the ABI Prism big dye terminator kit (PE Applied Biosystems, Foster City, CA) and the insert sequence was obtained on both strands using the ABI Prism 310 genetic analyzer. The DNA sequences were submitted to the BLAST program (Altschul *et al.* 1997) for similarity searches with the sequence databases. Sequence alignment and primer selection were performed using the GCG software (Devereux *et al.* 1984).

Virtual Northern analysis: Virtual Northern analysis was carried out to confirm the expression of the DD-PCR products. Full-length cDNAs were generated from 1 μg total RNA of each of the two midgut bulks used in the DD-PCR and of bulks from both infected and noninfected midguts for the two *A. aegypti* strains, RED and MOYO-R. The RNA was reverse-transcribed with the SMART PCR cDNA synthesis kit (Clontech) according to the manufacturer's instructions. The cDNAs were amplified from 1.5 μl of the first-strand cDNAs in a 100-μl reaction mixture with the PCR primer supplied with the kit. The PCR cycling profile was a first denaturation at 95° for 2 min followed by 18 cycles at 95° for 15 sec, 65° for 30 sec, and 68° for 6 min. Four hundred nanograms of the amplified cDNA products were resolved on a 1.2% TAE/agarose gel and subjected to Southern blotting and probe hybridizations as previously described (Severson 1997). The blot was successively hybridized with probes prepared from (1) a cloned DD-PCR product and (2) a RFLP marker clone (LF272) that represents partial sequence for the ribosomal protein S17 gene (RpS17; D. W. Severson, unpublished data).

Northern blotting: Tissue and/or developmental stage-specific expression was determined by standard Northern blotting. Ten micrograms of total RNA extracted from female guts, female carcasses following midgut removal, larvae, pupae, and males were separated by electrophoresis in 1.2% formaldehyde/agarose gels and transferred to Nylon membranes (Hybond, Amersham, Arlington Heights, IL). Hybridizations were performed at 42° in 50% formamide, 5× Denhardt's solution, 5× SSPE, 0.1% SDS, and 15 μg/ml denatured salmon sperm DNA. Membranes were washed to high stringency in 0.1× SSPE/0.5% SDS at 65° and visualized using a phosphorimaging system.

Semiquantitative RT-PCR: Because of the small amount of RNA recovered from midgut extractions, we did semiquantitative RT-PCR assays to assess differential expression. Total RNAs extracted from midguts dissected at different time points after an infective blood meal were used for expression analysis. One microgram of total RNA was reverse transcribed in a 20-μl reaction mixture containing 50 mm Tris-HCl pH 8.3, 3 mm $MgCl_2$, 75 mm KCl, 10 mm DTT, 500 μm of each dNTP, 20 pmol of oligo$(dT)_{18}$ (Clontech) and 200 units of Superscript II RNaseH$^-$ (GIBCO-BRL).

Quantification assays were investigated by multiplex RT-PCR, using the RpS17 gene sequence as the internal control for normalization. For each primer set, preliminary PCR amplifications were carried out under our standard conditions to determine the number of cycles necessary to attain visualized PCR products while avoiding saturation. Optimal cycle number was set at 22. Multiplex RT-PCRs were then performed with 1 μl of the RT products in a total volume of 25 μl in the presence of 50 mm Tris-HCl pH 8.3, 3 mm $MgCl_2$, 50 mm KCl, 400 μm of each dNTP, 0.25 units of *Taq* polymerase, 0.5 μCi [α-^{32}P]dCTP, 10 pmol of the DD-PCR product-specific primers and 20 pmol of the RpS17 primers. PCR products (3 μl) were separated by electrophoresis on 8% acrylamide gels. The gels were dried, exposed to phosphorimaging screens and visualized using a Storm 840 phosphorimaging system. The RT-PCR products were quantified using the ImageQuant 5.0 software (Molecular Dynamics).

Linkage analysis and genetic mapping: The cloned DD-PCR product was radiolabeled and used as a probe to the Southern blots of the F_1 intercross progeny as described above. Multipoint linkage analysis was conducted using the MAPMAKER computer package (Lander *et al.* 1987; Lincoln and Lander 1990). Recombination frequencies were converted into map distances (cM) using the Kosambi function (Kosambi 1944).

Competitive PCR: Strain-specific substitutions were confirmed by a competitive PCR assay. This assay was performed by the amplification of 1 ng of individual genomic DNA in a final volume of 25 μl using 50 mm Tris-HCl pH 8.3, 3 mm $MgCl_2$, 50 mm KCl, 400 μm of each dNTP, 0.25 units of *Taq* polymerase, 10 pmol of a reverse primer, 3 pmol of a forward primer and 20 pmol of an internal forward primer. PCRs were carried out at 95° for 2 min in a first denaturation, at 95° for 15 min, 65° for 1 min, and 72° for 2 min for 30 cycles, and then at 72° for 6 min for a final extension. PCR products were resolved on a 6% acrylamide gel, stained with ethidium bromide and visualized under UV light.

RESULTS

BSA-DD and identification of differentially expressed genes: Selective genotyping of F_1 intercross females was used to identify individuals homozygous at two RFLP loci closely flanking the major QTL *pgs 1*, LF181 and LF282, and heterozygous at two more distant RFLP loci, LF338 and LF272 (Figure 2). Two RNA bulked pools were prepared, each with midgut RNA from six individuals homozygous for the parental RED and MOYO-R genotypes at the loci flanking the QTL interval. The cDNAs from the RNA bulks were compared by DD-PCR to identify genes activated by the infected blood meal. Forty-six combinations of an arbitrary primer and an oligo(dT) primer were examined and 21 candidate differentially expressed cDNA products were isolated.

Two cDNA clones 456 and 508 bp in length were obtained with the same primer combination (AP8 and DT5) from the RED type bulk and the MOYO-R type bulk, respectively, that showed high similarity (97 and 96% identities, respectively) with an *A. aegypti* mucin-like (*AeIMUC1*) gene sequence (accession no. AF125984). The RED type sequence contains a deletion of a 51-bp motif at the 3′ end of the sequence. Virtual Northern blot analysis confirmed the *AeIMUC1* length polymorphism between the two *A. aegypti* strains (Figure 3A).

***AeIMUC1* polymorphism:** Primers (MLPF and MLPR, see Table 1) flanking the deletion polymorphism were designed and used to verify allele identities for the individuals bulked for the differential display analysis. All the mosquitoes pooled in the MOYO-R type bulk carried the MOYO-R allele (*AeIMUC^{M1}*, 242 bp), while those pooled in the RED type bulk carried the RED allele (*AeIMUC^{R1}*, 190 bp; data not shown).

PCR amplifications with the MLP primers were then performed on bulked DNA from several *A. aegypti* laboratory strains. Of interest, a third allele was identified

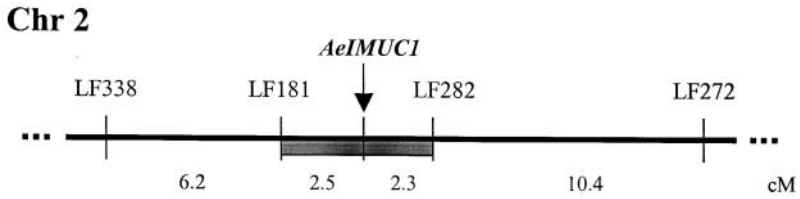

FIGURE 2.—Genetic mapping of *AeIMUC1*. Map distances of *MUC1* from the RFLP markers used to genotype the F_1 intercross progeny (n = 155 females) are indicated in centimorgans (cM). The *pgs 1* QTL interval is shown by the shaded area.

in two strains, the RED strain and the Formosus strain (Figure 3B). The new allele was intermediate in size (212 bp). A screening of random individuals from the RED strain was undertaken and indeed two alleles were segregating within the strain population. Subsequently, the third allele ($AeIMUC^{R2}$) was cloned and sequenced. Figure 4C shows the alignment of the three alleles. The $AeIMUC^{R2}$ allele has, when compared to the $AeIMUC^{M1}$ allele, a 30-bp deletion and the gap occurs completely within the same deleted region found in the $AeIMUC^{R1}$ allele. Within this polymorphic region, in the $AeIMUC^{M1}$ allele, a 9-bp repeat motif (AGTGGTTTC) flanks a 42-bp sequence and in the two other alleles the 3′ deletions involve this region. Whereas all the alleles have the 3′ repeat, the 5′ motif is absent in the $AeIMUC^{R1}$ allele. Thus the $AeIMUC^{R2}$ deletion occurs in the sequence flanked by the repeat motifs whereas the $AeIMUC^{R1}$ deletion consists of the full 42-bp sequence plus one repeat

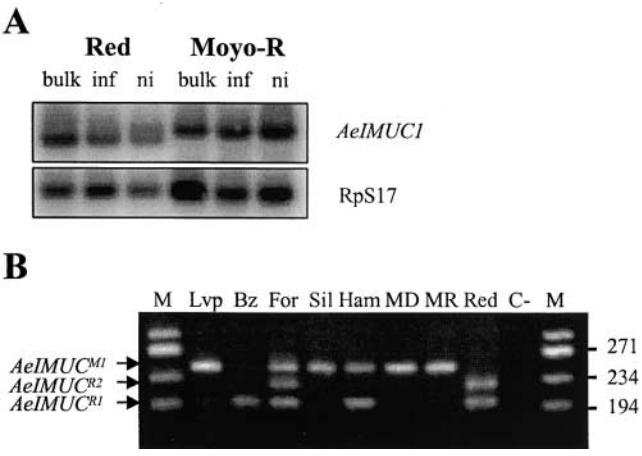

FIGURE 3.—*AeIMUC1* length polymorphism. (A) Virtual Northern blot of reverse-transcribed RNAs (~400 ng of cDNAs per lane) isolated from female midguts dissected 48 hr after a blood meal. Midguts were from the following sources: bulk, females used to prepare the RNA bulks; inf, females fed on infected chicks; ni, females fed on noninfected chicks. (Top) The blot was probed with ^{32}P-labeled *AeIMUC1* DD-PCR insert. The autoradiogram shows the length polymorphism between the two strains, RED and MOYO-R. (Bottom) The blot was stripped and rehybridized with the RpS17 ribosomal probe used as loading control. (B) Ethidium bromide-stained agarose gel showing left, *AeIMUC1* allelic polymorphism among several *A. aegypti* laboratory strains and right, *AeIMUC1* species specificity. *A. aegypti* strains: Lvp, Liverpool; Bz, Bronze; For, Formosus; Sil, Silver; Ham, Hamburg; MD, Moyo-in-Dry; MR, MOYO-R; Red, RED-EYE; C−, PCR negative control; M, Φ174 Hae III marker.

motif. Further, an adenosine residue is deleted in the $AeIMUC^{R1}$ allele 23 bases upstream from the deleted sequence. Also, as shown in Figure 4C, a 3-bp sequence reflects allele-specific substitutions. We also noted that the *AeIMUC1* gene from *A. aegypti* Rexville strain (RAYMS-KELLER *et al.* 2000) has the $AeIMUC^{R1}$ type allele.

Allele-specific single base substitutions were confirmed using a competitive PCR assay with primers (MSXF, X = M1, R1, or R2, see Table 1) designed with 3′ single base substitution anchors. PCR was performed on genomic DNA from individuals previously genotyped relative to the deletion polymorphism by adding one of the MSXF primers to the primers (MLPF, MLPR) flanking the length polymorphism (see MATERIALS AND METHODS). The MLPF primer was used at a limited amount (3 pmol) as a PCR control, to allow amplification even if the MSXF primer did not anneal. There was complete correlation between deletion polymorphisms and the expected amplicon with the corresponding MSXF primer (data not shown).

Cloning of *AeIMUC1* gene: The size of the *AeIMUC1* gene mRNA as detected on virtual Northern blots was estimated to be ~1200 bp. To facilitate cloning of the complete putative coding sequence of each allele, primers (MUCF, MUCR, see Table 1) were designed on the basis of the DD-PCR insert's similarity to the *A. aegypti* mucin-like protein published sequence. Full gene sequences for each allele were obtained by PCR amplifications using the full-length cDNAs generated in the virtual Northern procedure from both *A. aegypti* strains. The 3′ and 5′ ends were obtained by using a combination of an internal primer and one of the two primers used in the SMART PCR cDNA synthesis kit, respectively MUCIPF/CDS and MUCIPR/SMO (see Table 1).

Sequences of 1020, 1018, and 1072 bp in length were obtained for the $AeIMUC^{R1}$, $AeIMUC^{R2}$, and $AeIMUC^{M1}$ alleles, respectively. Each sequence includes a complete open reading frame encoding a putative protein, of 275 amino acids (aa) for the $AeIMUC^{R1}$ allele, 273 aa for the $AeIMUC^{R2}$ allele, and 271 aa for the $AeIMUC^{M1}$ allele (Figure 4A). The $AeIMUC^{M1}$ sequence terminates earlier when compared to the two other alleles because of the trinucleotide substitution which results in a TAA stop codon at peptide position 272 (Figure 4C). The adenosine residue deletion observed in the $AeIMUC^{R1}$ allele results in a frameshift that produces a stop codon (TAG) just downstream from this single base deletion. With the $AeIMUC^{R2}$ allele, a TAG stop codon occurs upstream of the 30-bp deletion. A putative transcription initiator

TABLE 1

Oligonucleotide primers used to characterize the *AeIMUC1* gene

Primer	Length	Sequence	Specificity
MUCF	22-mer	5′-GCTGTCCACCATCAATAGATTG-3′	MUC 5′ end
MUCR	22-mer	5′-CAATACACTGATAACATCTCTC-3′	MUC 3′ end
MLPF	21-mer	5′-GCTGGACTCCACTGGAATAAG-3′	MUC 3′ deletion
MLPR	20-mer	5′-TGAATGTGTCATCGTCATCG-3′	MUC 3′ deletion
MUCIPF	20-mer	5′-CAAAGTCTACGTATGCACCC-3′	MUC internal primer
MUCIPR	21-mer	5′-CTGTTGATTCCAGTGAAGTCC-3′	MUC internal primer
MSM1F	21-mer	5′-AGGCTTCAAACACTCGAATTA-3′	MUC^{M1} 3′ substitutions
MSR1F	21-mer	5′-AGTCTTCAAACACTCGAAACC-3′	MUC^{R1} 3′ substitutions
MSR2F	21-mer	5′-AGGCTTCAAACACTCGAAATC-3′	MUC^{R2} 3′ substitutions

sequence (TCAAT) and a putative polyadenylation signal (AATAAA) appear in each of the three alleles, located respectively at 22 bp of the 5′ end and at 19 bp upstream from the poly(A) tail (Figure 5).

The complete nucleotide sequences of *AeIMUC1* for the three alleles revealed that the $AeIMUC^{R2}$ allele has two deletions: the 30-bp deletion at the 3′ end of the sequence (see above) and a 24-bp deletion in the mucin domain. As shown in Figure 4B, if compared to the $AeIMUC^{M1}$ allele, the 24-bp deletion involves a 13-bp repeat motif and the 11-bp sequence located between the two repeats. The corresponding region in the $AeIMUC^{R1}$ allele has four single nucleotide substitutions that change the first repeat motif.

Comparison of the nucleotide sequences for the three alleles revealed multiple point mutations. A total of 46 single nucleotide polymorphisms (SNPs) were found. The SNP distribution among the *AeIMUC1* alleles is as follows: 10 for the MUC^{M1} allele, 21 for the $AeIMUC^{R1}$ allele, and 15 for $AeIMUC^{R2}$ allele (Figure 5; GenBank accession nos. AF308863 and AF308864). Some, but not all of them, are nonsynonymous cSNPs and thus, as shown in Figure 4A, 22 amino acid substitutions are found.

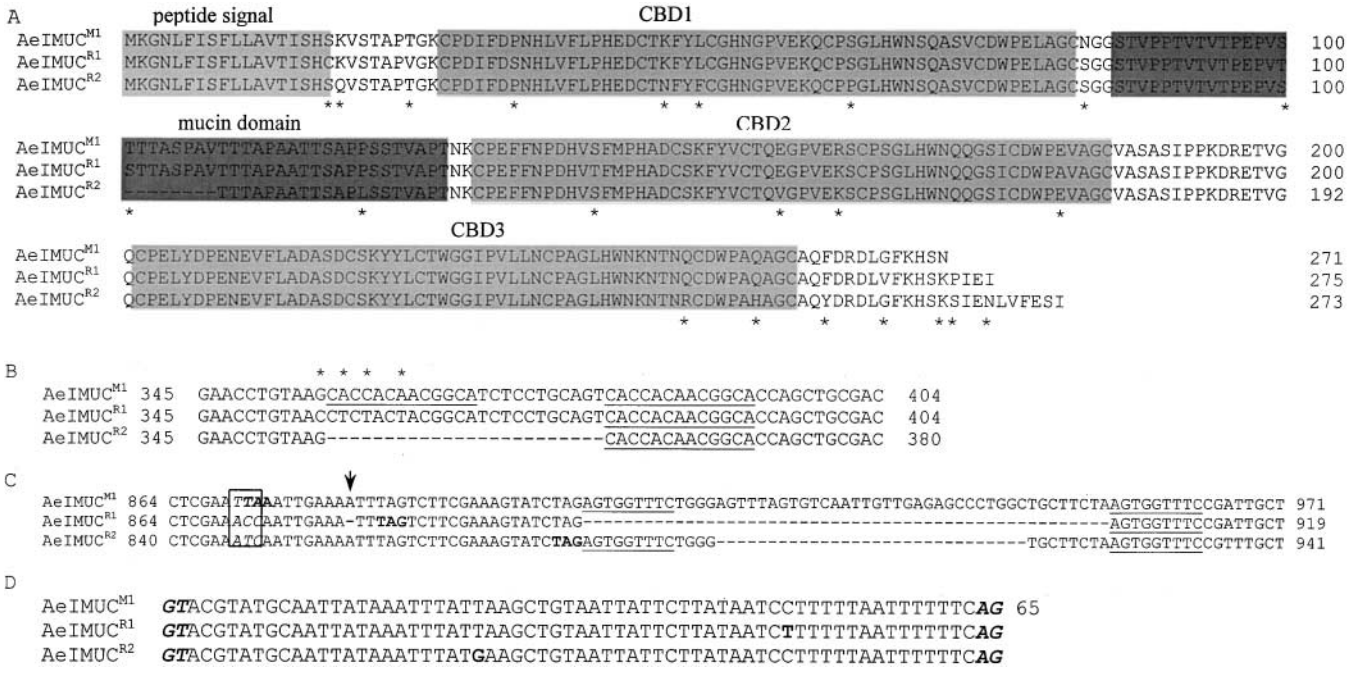

FIGURE 4.—*AeIMUC1* allelic polymorphisms. (A) Amino acid sequence alignment of the three *AeIMUC1* alleles. Asterisks mark allele-specific substitutions. The different protein domains are shaded and indicated. (B) Nucleotide sequence comparison at the deletion within the mucin domain. The repeat motif is underlined and the single nucleotide substitutions are marked with asterisks. Numbers indicate the position in the cDNA nucleotide sequence. (C) Nucleotide sequence comparison showing the 3′ end deletion polymorphism. The adenosine deletion in the $AeIMUC^{R1}$ allele is indicated by an arrow. The termination codon for each allele is in boldface type. The trinucleotide substitution is boxed. The repeat motif flanking the deleted area is underlined. (D) Nucleotide sequence comparison of the 65-bp intron. Single nucleotide substitutions are in boldface type. The splice junctions are italicized.

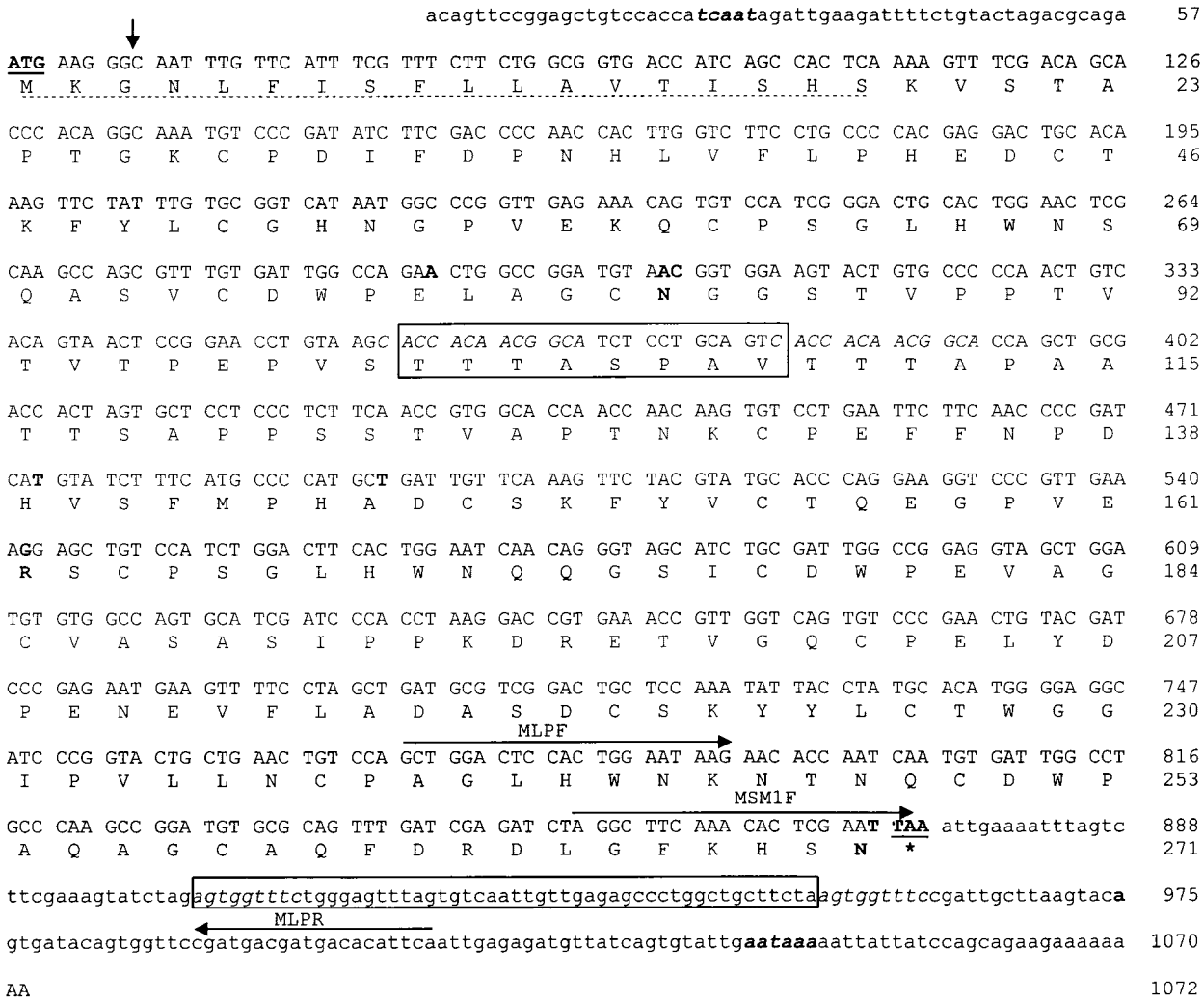

FIGURE 5.—Nucleotide and deduced amino acid sequences of *AeIMUC*^{M1} cDNA. The 5′ and 3′ noncoding regions are represented by lowercase type. A putative transcription initiator sequence (tcaat) and a potential polyadenylation signal (aataaa) are in boldface and italic. The translation initiation codon and the termination codon are in boldface type and underlined. The predicted peptide signal sequence is underlined with a broken line. The regions showing deletion polymorphisms in the two other alleles are boxed and the repeat motifs are italicized. Primer set (MLPF, MLPR) used to determine allele identity and primer designed for the competitive assay (MSM1F) are indicated above the sequence. The SNPs specific to the *AeIMUC*^{M1} allele are in boldface type. The location of the intron in the corresponding genomic sequence is indicated by an arrow.

Domain organization of *AeIMUC1*: BLAST search with the full-length *AeIMUC1* amino acid sequence revealed high similarities to peritrophic matrix proteins and insect chitinases. The deduced amino acid sequence of *AeIMUC1* contains several conserved domains. The N-terminal amino acid sequence contains a signal peptide of 18 amino acids, typical of a secretory protein. A central core presents characteristic features of a mucin-like domain (GENDLER and SPICER 1995). The amino acid sequence is rich in threonine, proline, alanine, valine, and serine (32.5, 20.9, 16.3, 14.0, 14.0%, respectively). Three imperfect tandem repeats (TTTASPAV) are present in the *AeIMUC*^{M1} and *AeIMUC*^{R1} alleles while only two repeats are present in the *AeIMUC*^{R2} allele (Figure 4A). For the *AeIMUC*^{R2} allele, the 24-bp deleted sequence represents the first amino acid tandem repeat. As predicted by a search on the *NetOglyc* WWW server (HANSEN *et al.* 1998), all threonine and serine residues of this mucin domain are potential *O*-glycosylation sites. The predicted molecular mass of the peptide is 29.2 kD, but the likely presence of numerous *O*-linked carbohydrates suggests that the glycoprotein mass might be higher.

AeIMUC1 sequence also contains three putative chitin-binding domains (CBDs). Chitin-binding domains are characterized by positional conservation of six cysteines and aromatic residues (SHEN and JACOBS-LORENA 1999). The six cysteine residues form disulfide bonds and the conserved aromatic amino acids could be involved in binding specificity. The first putative CBD of *AeIMUC1* peptide is located at the N terminus, upstream to the mucin domain and the two others are at the C terminus, downstream to the mucin domain (Figure

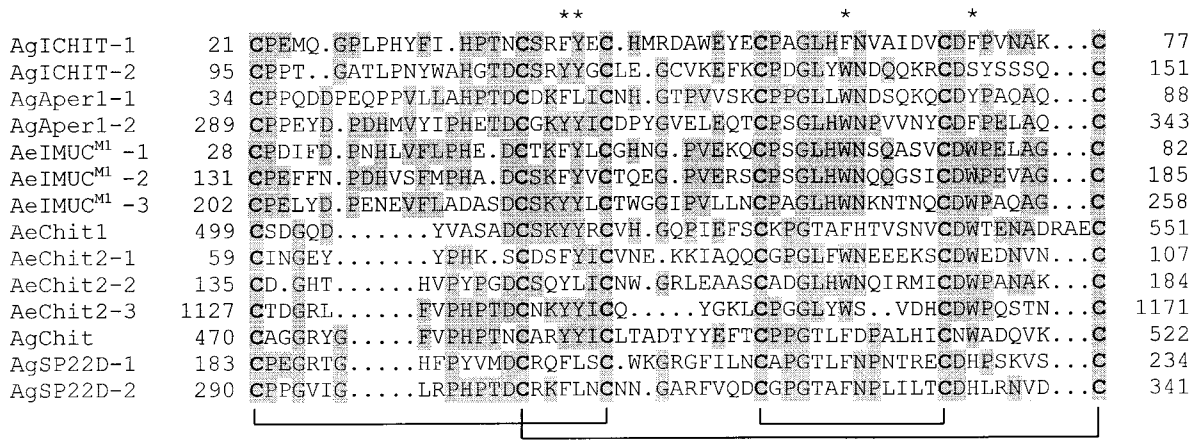

FIGURE 6.—Alignment of the *AeIMUC*^{M1} putative chitin-binding domains with homologous sequence motifs from *A. gambiae ICHIT* protein (*AgICHIT-1* and *AgICHIT-2*), *A. gambiae* peritrophin 1 (*AgAper1-1* and *AgAper1-2*), *A. aegypti* chitinase 1 (*AeChit1*), *A. aegypti* chitinase 2 (*AeChit2-1*, *AeChit2-2*, and *AeChit2-3*), *A. gambiae* chitinase (*AgChit*), and *A. gambiae* serine protease *Sp22D* (*AgSP22D-1* and *AgSP22D-2*). Conserved cysteines are in boldface type and the disulfide bonds are illustrated at the bottom, according to SHEN and JACOBS-LORENA (1999). Conserved aromatic amino acids are marked with asterisks.

4A). The three CBDs share significant similarity with *Anopheles gambiae* peritrophin 1 (GenBank accession no. AAC39127), with *A. aegypti* chitinase (GenBank accession no. T14075), and with *AgICHIT* protein, which is an *A. gambiae* intestinal protein composed of two CBDs separated by a mucin domain (GenBank accession no. CAA09389). Figure 6 represents the sequence alignment of CBDs found in *A. gambiae* and *A. aegypti* proteins. *AeIMUC1* CBD motifs share highest homology with *Ag-Aper*1, a major protein of the *A. gambiae* peritrophic matrix, and it is likely that the *AeIMUC1* protein is also a constituent of the peritrophic matrix in *A. aegypti*.

Genomic sequence: Genomic DNA fragments specific for *MUC1* were produced by amplification of gDNA from individuals previously genotyped relative to the deletion polymorphism with primers (MUCF, MUCR) flanking the open reading frame (ORF). As compared to cDNA amplification products, a larger amplicon was obtained for each of the three alleles, suggesting the presence of introns in the genomic DNA. Genomic fragments when cloned and sequenced revealed a 65-bp intron with the GU-AG feature characteristic of eukaryotic nuclear pre-mRNA. The 5′ splice site is located four amino acids downstream to the start codon (Figure 5). Sequences for the three alleles are similar; Figure 4D shows the substitutions between the three alleles.

Expression of *AeIMUC1*: Developmental stage and tissue-specific expression of *AeIMUC1* were investigated by Northern blot analysis using total RNA from larvae, pupae, female carcasses (whole body minus midgut), female midguts, and males. *AeIMUC1* was detected only in RNA from female midguts (Figure 7), suggesting that *AeIMUC1* gene expression is female midgut specific.

AeIMUC1 gene expression following *P. gallinaceum* infection was examined by semiquantitative RT-PCR analyses on total RNAs from midguts dissected 24, 48, and 72 hr and 7 days after an infective blood meal. RNAs extracted from midguts 48 hr after a noninfective feeding and from midguts of nonfed females were also screened, as *AeIMUC1* expression could be induced by parasite ingestion or by the blood meal. The ratio of MLP PCR products/RpS17 PCR products was plotted against time after the blood meal for three independent experiments. Results were analyzed initially by a two-way ANOVA. *AeIMUC1* expression levels were similar for both *A. aegypti* strains ($P > 0.05$) while significant differences in expression were observed for time after an infected blood meal ($P < 0.05$). No significant interaction effects were observed. We therefore pooled data across strains and the results were analyzed by a one-way ANOVA. Significant differences in time after blood meal ingestion were evident ($P < 0.05$); gene expression decreased with time after the blood meal ingestion (Figure 8A).

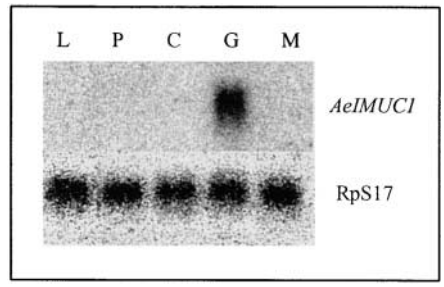

FIGURE 7.—Developmental and tissue-specific expression of *MUC1*. (Top) Northern analysis of ^{32}P-labeled *AeIMUC1* DD-PCR insert on total RNAs (~10 μg per lane) isolated from different developmental stages and tissues (L, larvae; P, pupae; C, female carcasses; G, female midguts; M, males). (Bottom) The blot was stripped and rehybridized with the RpS17 ribosomal probe used as loading control.

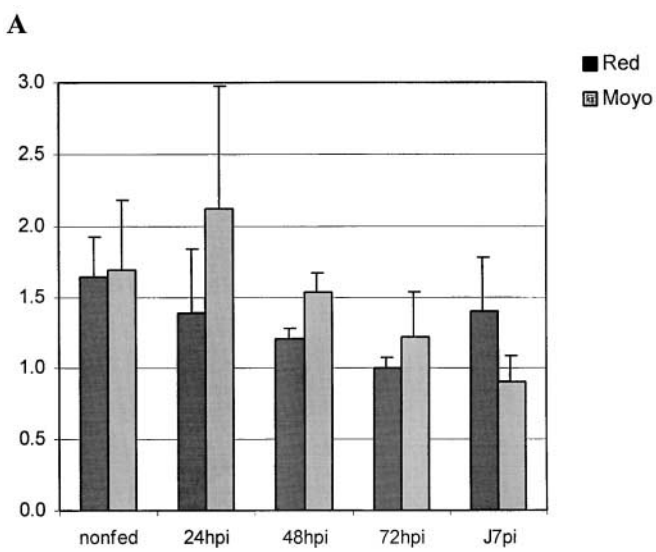

FIGURE 8.—Expression analysis of *AeIMUC1* following exposure to a parasite-infected blood meal. Midgut RNAs from the susceptible RED and the resistant MOYO-R *A. aegypti* strains at different times following blood-feeding were used for semiquantitative RT-PCR standardized against RpS17. (A) Female midguts at 24, 48, and 72 hr and 7 days postfeeding on an infected blood meal (pi). (B) Female midguts at 48 hr following a noninfected (pf) and an infected (pi) blood meal. Values are means and standard deviations for three independent experiments ($n = 15$ pooled midguts/experiment).

We also compared *AeIMUC1* expression levels at 48 hr following an uninfective *vs.* infective blood meal (Figure 8B). Because we observed no significant differences in expression between strains, data for the two strains were pooled and subjected to a *t*-test. We observed a significant difference ($P = 0.008$) in expression relative to blood meal status; *AeIMUC1* expression levels remained higher at 48 hr postfeeding among individuals that received an infective blood meal.

Genetic mapping: Southern blots of the F_1 intercross progeny used for the BSA-DD procedure were probed with the *AeIMUC1* fragment obtained by DD-PCR to genetically determine its map position. Recombination frequencies of *AeIMUC1* and the RFLP markers previously mapped in the F_1 intercross population localized the gene between two markers (LF181 and LF282) flanking the major QTL (*pgs 1*) determining *P. gallinaceum* susceptibility in *A. aegypti* (Figure 2).

DISCUSSION

The development of detailed genetic linkage maps using DNA-based markers has facilitated the dissection of complex traits into discrete components referred to as QTL, but the actual isolation of the associated genes remains a significant challenge. The integrated BSA-DD approach described in this article provides a rapid and accurate method to directly isolate candidate genes associated with QTL influencing a phenotype of interest such as pathogen/vector interactions. The procedure requires a population segregating for a genome region of interest and the ability to isolate both DNA and RNA from individuals within this population. As in classical BSA analysis, molecular markers defining a target region are used to identify individuals homozygous at loci flanking the target interval and heterozygous at more distant loci. However, with the BSA-DD approach, RNA from the selected individuals is then used to prepare two pools, each representing one of the parental genotypes across the target interval. In theory the two bulks should contain identical RNA species except for those RNAs differentially expressed by genes within the genome region of interest. Comparisons of the RNA bulks should identify polymorphisms associated with genes located in the targeted region. Additionally, RNA can be extracted from specific tissues considered to be likely sites for differential expression associated with QTL.

We demonstrated the utility of the BSA-DD approach for the isolation of differentially expressed RNAs within the genome region containing the major QTL, *pgs 1*, determining *P. gallinaceum* susceptibility in the mosquito *A. aegypti*. We characterized a mucin-like protein (*AeIMUC1*) that is adult female midgut specific and shares similarities with PM proteins. The structure of *AeIMUC1*, with three cysteine-rich domains and a mucin domain, strongly suggests that this protein is a mucin-like peritrophin of the adult female *A. aegypti* mosquito. The gene maps within the *pgs 1* QTL interval, shows significant differences in expression following uninfected *vs.* parasite infected blood meals, and reflects allelic length polymorphism between our susceptible and resistant *A. aegypti* mosquito strains, suggesting that it could be directly involved in *P. gallinaceum* susceptibility. The mucin-like protein, *AeIMUC1*, recently identified by others in another *A. aegypti* strain was shown to be induced in the larval midgut after heavy metal exposure as well as in the adult female midgut within the first 6 hr after blood meal ingestion (RAYMS-KELLER *et al.* 2000). These data are in accordance with our results. The fact that in our experiments no overexpression of *AeIMUC1* was detected at 24 hr after an infected blood meal suggests that the mRNA is rapidly degraded.

Two types of PMs are defined in insects, relating to their site of synthesis. Type 1 PM is secreted by midgut epithelial cells in many adult blood-feeding insects, whereas type 2 is synthesized by specialized cells within

the cardia, an organ located in the anterior part of the midgut. The distinction between the two PM types is not clear at the molecular level. Typically, mosquitoes produce a different PM type at different life stages, *e.g.*, type 2 PM during larval life and type 1 PM during adult life. Most insect PM proteins characterized to date have been isolated from larval stages (Elvin *et al.* 1996; Casu *et al.* 1997; Wang and Granados 1997). Most of these PM proteins (called peritrophins) also share common properties with mammalian mucins (Tellam *et al.* 1999) and they are characterized by the presence of both cysteine-rich or chitin-binding domains and proline/threonine stretches. Similarities in their structural organization and location (covering epithelial cells) suggest that both proteins have analogous functions, particularly to protect the midgut epithelium. None of the PM proteins from adult-stage insects described so far show all characteristic features of mucin-like peritrophins. The only peritrophin characterized previously from blood-fed adult mosquitoes is *Ag-Aper*1 from *A. gambiae*, which has two CBDs but no mucin domain (Shen and Jacobs-Lorena 1998). Other adult midgut proteins have been described but their association with the PM has not been demonstrated.

The *AeIMUC1* protein contains three CBDs that show high sequence similarity to each other. Presence of CBDs suggests that the protein has the capacity to bind chitin within the PM. CBDs are commonly found in both insect PM proteins and invertebrate chitinases and share amino acid sequence similarities (Shen and Jacobs-Lorena 1999). They are cysteine rich and have highly conserved aromatic residues. In CBDs of all related genes six cysteine residues can be aligned and likely allow the formation of disulfide bonds. Disulfide bonds help to maintain a digestive protease-resistant structure while the aromatic residues are presumed to determine binding specificity (Elvin *et al.* 1996; Wang and Granados 1997; Shen and Jacobs-Lorena 1999). *AeIMUC1* CBDs show high similarity with *Ag-Aper*1 CBDs, although *MUC1* contains three CBDs while *Ag-Aper*1 contains only two CBDs (Shen and Jacobs-Lorena 1998). *A. aegypti* chitinase also has three CBDs with significant amino acid sequence similarity to *AeIMUC1* CBDs. *AeIMUC1* CBDs show greater homology to *Ag-Aper*1 domains than to *A. aegypti* chitinase domains, and it is unlikely that *AeIMUC1* protein and *A. aegypti* chitinase interact. They probably have synergistic functions: *AeIMUC1* could promote the formation of PM structure by connecting chitin fibers, whereas *A. aegypti* chitinase is likely involved in PM degradation. Multiple CBDs are common in insect PM proteins and invertebrate chitinases and it has been argued that they result from gene duplication (Shen and Jacobs-Lorena 1999).

It has been suggested previously that a carbohydrate might be involved in vector-parasite specificity by enabling the ookinete to recognize the peritrophic matrix and/or the midgut epithelium (Billingsley and Rudin 1992; Ramasamy *et al.* 1997; Zieler *et al.* 1999). In adult female *A. aegypti*, the PM forms after the blood meal and is complete after 12 hr (Richards and Richards 1977). The ookinetes begin to penetrate the PM 24 hr after feeding, after the membrane is completely formed (Sieber *et al.* 1991). Several studies suggest that while the PM is a physical barrier for parasite transmission (see review in Shahabuddin 1998) it is not an absolute barrier and instead it reduces the intensity of infection (Billingsley and Rudin 1992). The PM may act as a recognition site for the penetrating ookinetes, by exposing specific carbohydrate ligands to the parasites (Billingsley 1994). It is known that *P. gallinaceum* ookinetes produce and secrete a chitinase (Huber *et al.* 1991) that is secreted as a proenzyme and is activated by a mosquito midgut trypsin (Shahabuddin *et al.* 1993, 1995). During ookinete penetration through the PM the membrane is disrupted only around the invading point (Sieber *et al.* 1991) and inhibitors of chitinase block parasite transmission (Shahabuddin *et al.* 1993, 1996). Therefore once the PM is encountered and recognized, the parasites use their own chitinase to cross it. The *MUC1* glycoprotein with high *O*-glycosylated sites may be a likely candidate for a PM recognition molecule; the CBDs allow the protein to crosslink with chitin fibrils and the mucin domain exposes carbohydrates to the endoperitrophic space.

The inter- and intrastrain allelic polymorphism observed with the *AeIMUC1* gene and its genome location within the *pgs 1* QTL interval are suggestive that it may play a significant role in *A. aegypti* infection by *P. gallinaceum* and, ultimately, vector competence to transmit the parasite to vertebrates. However, these results are simply correlative and do not in themselves confirm this hypothesis. Obviously, this needs to be tested directly using a gene expression system such as the *Sindbis* virus-transducing vector (Olson *et al.* 2000). SNP-based association studies should also be done to determine the potential influence of individual sequence variants on the susceptible/resistant phenotype.

Identification of differentially expressed genes is of great importance, as they constitute candidate genes for use in developing effective control strategies for vector-borne diseases. Although several techniques that produce differential transcripts between two populations of RNAs exist (Lee *et al.* 1991; Hubank and Schatz 1994; Prashar and Weissman 1996; Suzuki *et al.* 1996), RNA-based methods are often limited for mosquito studies by the availability of sufficient material. The RNA differential display method overcomes this limitation, as only 1 μg of total RNA is sufficient for use as starting material. The main drawbacks reported with this technique are the high levels of false positives and biases for high copy number genes (Liang *et al.* 1993; Bertioli *et al.* 1995; Luce and Burrows 1998). In addition, this method is likely to miss mutations that affect phenotype expression but not transcription levels. The more recent

method of suppression subtractive hybridization (SSH; Diatchenko *et al.* 1996) offers an alternative for identification of differentially expressed genes. The SSH method incorporates normalization and subtraction in a single procedure that facilitates isolation of cDNAs representing rare transcripts and is also appropriate for an integrated BSA-SSH approach.

Current proposed genetic-control strategies for mosquitoes are based on modification of the capacity of the natural vector to support parasite development (Collins and Paskewitz 1995). Germline transformation of insect vectors has already been achieved (Jasinskiene *et al.* 1998; Catteruccia *et al.* 2000), so the identification of transmission-blocking genes remains a primary goal in efforts to engineer malaria-refractory mosquitoes. At present, no gene has been shown to be directly correlated with genetic refractoriness. Targeting differential gene expression in genome regions associated with parasite susceptibility could allow for the rapid and efficient identification of the associated genes.

We have shown that the BSA-DD approach provides an efficient method for the identification of putative differentially expressed genes within a diploid organism for which molecular markers delimiting QTL exist. The technique should be useful for the identification of genes that play key roles in a wide range of systems, including plants and animals.

We are grateful to Jeanne Romero-Severson for helpful discussions. The sequences reported in this article have been deposited in the GenBank database and assigned the following accession numbers: AeIMUC^{M1}, AF308862; AeIMUC^{R1}, AF308863; AeIMUC^{R2}, AF308864. This work was supported by a grant (AI 33127) from the National Institutes of Health.

LITERATURE CITED

Altschul, S. F., T. L. Madden, A. A. Schaffer, J. Zhang, Z. Zhang *et al.*, 1997 Gapped BLAST and PSI-BLAST: a new generation of protein database search programs. Nucleic Acids Res. **25:** 3389–3402.

Bertioli, D. J., U. H. Schlichter, M. J. Adams, P. R. Burrows, H. H. Steinbiss *et al.*, 1995 An analysis of differential display shows a strong bias towards high copy number mRNAs. Nucleic Acids Res. **23:** 4520–4523.

Billingsley, P. F., 1994 Vector-parasite interactions for vaccine development. Int. J. Parasitol. **24:** 53–58.

Billingsley, P. F., and W. Rudin, 1992 The role of the mosquito peritrophic membrane in bloodmeal digestion and infectivity of *Plasmodium* species. J. Parasitol. **78:** 430–440.

Casu, R., C. Eisemann, R. Pearson, G. Riding, I. East *et al.*, 1997 Antibody-mediated inhibition of the growth of larvae from an insect causing cutaneous myiasis in a mammalian host. Proc. Natl. Acad. Sci. USA **94:** 8939–8944.

Catteruccia, F., T. Nolan, C. Blass, H. M. Muller, A. Crisanti *et al.*, 2000 Toward *Anopheles* transformation: Minos element activity in anopheline cells and embryos. Proc. Natl. Acad. Sci. USA **97:** 2157–2162.

Collins, F. H., and S. M. Paskewitz, 1995 Malaria: current and future prospects for control. Annu. Rev. Entomol. **40:** 195–219.

Crampton, J. M., A. Warren, G. J. Lycett, M. A. Hughes, I. P. Comley *et al.*, 1994 Genetic manipulation of insect vectors as a strategy for the control of vector-borne disease. Ann. Trop. Med. Parasitol. **88:** 3–12.

Devereux, J., P. Haeberli and O. Smithies, 1984 A comprehensive set of sequence analysis programs for the VAX. Nucleic Acids Res. **12:** 387–395.

Diatchenko, L., Y. F. Lau, A. P. Campbell, A. Chenchik, F. Moqadam *et al.*, 1996 Suppression subtractive hybridization: a method for generating differentially regulated or tissue-specific cDNA probes and libraries. Proc. Natl. Acad. Sci. USA **93:** 6025–6030.

Dimopoulos, G., A. Richman, A. della Torre, F. C. Kafatos and C. Louis, 1996 Identification and characterization of differentially expressed cDNAs of the vector mosquito, *Anopheles gambiae*. Proc. Natl. Acad. Sci. USA **93:** 13066–13071.

Elvin, C. M., T. Vuocolo, R. D. Pearson, I. J. East, G. A. Riding *et al.*, 1996 Characterization of a major peritrophic membrane protein, peritrophin-44, from the larvae of *Lucilia cuprina*. cDNA and deduced amino acid sequences. J. Biol. Chem. **271:** 8925–8935.

Frost, M. R., and J. A. Guggenheim, 1999 Prevention of depurination during elution facilitates the reamplification of DNA from differential display gels. Nucleic Acids Res. **27:** e6.

Gendler, S. J., and A. P. Spicer, 1995 Epithelial mucin genes. Annu. Rev. Physiol. **57:** 607–634.

Giovannoni, J. J., R. A. Wing, M. W. Ganal and S. D. Tanksley, 1991 Isolation of molecular markers from specific chromosomal intervals using DNA pools from existing mapping populations. Nucleic Acids Res. **19:** 6553–6558.

Hansen, J. E., O. Lund, N. Tolstrup, A. A. Gooley, K. L. Williams *et al.*, 1998 NetOglyc: prediction of mucin type O-glycosylation sites based on sequence context and surface accessibility. Glycoconj. J. **15:** 115–130.

Hubank, M., and D. G. Schatz, 1994 Identifying differences in mRNA expression by representational difference analysis of cDNA. Nucleic Acids Res. **22:** 5640–5648.

Huber, M., E. Cabib and L. H. Miller, 1991 Malaria parasite chitinase and penetration of the mosquito peritrophic membrane. Proc. Natl. Acad. Sci. USA **88:** 2807–2810.

Jasinskiene, N., C. J. Coates, M. Q. Benedict, A. J. Cornel, C. S. Rafferty *et al.*, 1998 Stable transformation of the yellow fever mosquito, *Aedes aegypti*, with the *Hermes* element from the housefly. Proc. Natl. Acad. Sci. USA **95:** 3743–3747.

Kang, D., G. Liu, H. Gunne and H. Steiner, 1996 PCR differential display of immune gene expression in *Trichoplusia ni*. Insect Biochem. Mol. Biol. **26:** 177–184.

Kilama, W. L., and G. B. Craig, Jr., 1969 Monofactorial inheritance of susceptibility to *Plasmodium gallinaceum* in *Aedes aegypti*. Ann. Trop. Med. Parasitol. **63:** 419–432.

Kohroki, J., M. Tsuchiya, S. Fujita, T. Nakanishi, N. Itoh *et al.*, 1999 A novel strategy for identifying differential gene expression: an improved method of differential display analysis. Biochem. Biophys. Res. Commun. **262:** 365–367.

Kosambi, D. D., 1944 The estimation of map distance from recombination values. Ann. Eugen. **12:** 172–175.

Lander, E. S., P. Green, J. Abrahamson, A. Barlow, M. J. Daly *et al.*, 1987 MAPMAKER: an interactive computer package for constructing primary genetic linkage maps of experimental and natural populations. Genomics **1:** 174–181.

Lee, S. W., C. Tomasetto and R. Sager, 1991 Positive selection of candidate tumor-suppressor genes by subtractive hybridization. Proc. Natl. Acad. Sci. USA **88:** 2825–2829.

Lehane, M. J., A. B., and P. F. Billingsley, (Editors), 1996 *Biology of the Insect Midgut*. Chapman & Hall, New York.

Liang, P., and A. B. Pardee, 1992 Differential display of eukaryotic messenger RNA by means of the polymerase chain reaction. Science **257:** 967–971.

Liang, P., L. Averboukh and A. B. Pardee, 1993 Distribution and cloning of eukaryotic mRNAs by means of differential display: refinements and optimization. Nucleic Acids Res. **21:** 3269–3275.

Lincoln, S. E., and E. S. Lander, 1990 Mapping genes controlling quantitative traits using MAPMAKER/QTL. Whitehead Institute for Biomedical Research, Cambridge, MA.

Luce, M. J., and P. D. Burrows, 1998 Minimizing false positives in differential display. Biotechniques **24:** 766–768, 770.

Michelmore, R. W., I. Paran and R. V. Kesseli, 1991 Identification of markers linked to disease-resistance genes by bulked segregant analysis: a rapid method to detect markers in specific genomic regions by using segregating populations. Proc. Natl. Acad. Sci. USA **88:** 9828–9832.

Olson, K. E., K. M. Myles, R. C. Seabaugh, S. Higgs, J. O. Carlson

et al., 2000 Development of a *Sindbis* virus expression system that efficiently expresses green fluorescent protein in midguts of *Aedes aegypti* following *per os* infection. Insect Mol. Biol. **9:** 57–65.

Peters, W., (Editor), 1992 *Peritrophic membranes.* Springer-Verlag, Berlin.

Prashar, Y., and S. M. Weissman, 1996 Analysis of differential gene expression by display of 3′ end restriction fragments of cDNAs. Proc. Natl. Acad. Sci. USA **93:** 659–663.

Ramasamy, R., I. C. Wanniarachchi, K. A. Srikrishnaraj and M. S. Ramasamy, 1997 Mosquito midgut glycoproteins and recognition sites for malaria parasites. Biochim. Biophys. Acta **1361:** 114–122.

Rayms-Keller, A., M. McGaw, C. Oray, J. O. Carlson and B. J. Beaty, 2000 Molecular cloning and characterization of a metal responsive *Aedes aegypti* intestinal mucin cDNA. Insect Mol. Biol. **9:** 419–426.

Richards, A. G., and P. A. Richards, 1977 The peritrophic membranes of insects. Annu. Rev. Entomol. **22:** 219–240.

Sambrook, J., E. F. Fritsch and T. Maniatis, 1989 *Molecular Cloning: A Laboratory Manual.* Cold Spring Harbor Laboratory Press, Cold Spring Harbor, NY.

Schroeder, A. A., C. E. Lawrence and M. S. Abrahamsen, 1999 Differential mRNA display cloning and characterization of a *Cryptosporidium parvum* gene expressed during intracellular development. J. Parasitol. **85:** 213–220.

Severson, D. W., 1997 RFLP analysis of insect genomes, pp. 309–320 in *The Molecular Biology of Insect Disease Vectors*, edited by J. M. Crampton, C. B. Beard and C. Louis. Chapman & Hall, London.

Severson, D. W., A. Mori, Y. Zhang and B. M. Christensen, 1993 Linkage map for *Aedes aegypti* using restriction fragment length polymorphisms. J. Hered. **84:** 241–247.

Severson, D. W., V. Thathy, A. Mori, Y. Zhang and B. M. Christensen, 1995 Restriction fragment length polymorphism mapping of quantitative trait loci for malaria parasite susceptibility in the mosquito *Aedes aegypti.* Genetics **139:** 1711–1717.

Severson, D. W., D. Zaitlin and V. A. Kassner, 1999 Targeted identification of markers linked to malaria and filarioid nematode parasite resistance genes in the mosquito *Aedes aegypti.* Genet. Res. **73:** 217–224.

Shahabuddin, M., 1998 *Plasmodium* ookinete development in the mosquito midgut: a case of reciprocal manipulation. Parasitology **116:** S83–S93.

Shahabuddin, M., T. Toyoshima, M. Aikawa and D. C. Kaslow, 1993 Transmission-blocking activity of a chitinase inhibitor and activation of malarial parasite chitinase by mosquito protease. Proc. Natl. Acad. Sci. USA **90:** 4266–4270.

Shahabuddin, M., M. Criscio and D. C. Kaslow, 1995 Unique specificity of *in vitro* inhibition of mosquito midgut trypsin-like activity correlates with *in vivo* inhibition of malaria parasite infectivity. Exp. Parasitol. **80:** 212–219.

Shahabuddin, M., F. J. Lemos, D. C. Kaslow and M. Jacobs-Lorena, 1996 Antibody-mediated inhibition of *Aedes aegypti* midgut trypsins blocks sporogonic development of *Plasmodium gallinaceum.* Infect. Immun. **64:** 739–743.

Shen, Z., and M. Jacobs-Lorena, 1998 A type I peritrophic matrix protein from the malaria vector *Anopheles gambiae* binds to chitin. Cloning, expression, and characterization. J. Biol. Chem. **273:** 17665–17670.

Shen, Z., and M. Jacobs-Lorena, 1999 Evolution of chitin-binding proteins in invertebrates. J. Mol. Evol. **48:** 341–347.

Sieber, K. P., M. Huber, D. Kaslow, S. M. Banks, M. Torii *et al.*, 1991 The peritrophic membrane as a barrier: its penetration by *Plasmodium gallinaceum* and the effect of a monoclonal antibody to ookinetes. Exp. Parasitol. **72:** 145–156.

Suzuki, H., T. Yaoi, J. Kawai, A. Hara, G. Kuwajima *et al.*, 1996 Restriction landmark cDNA scanning (RLCS): a novel cDNA display system using two-dimensional gel electrophoresis. Nucleic Acids Res. **24:** 289–294.

Tellam, R. L., (Editor), 1996 The peritrophic matrix, in *Biology of the Insect Midgut.* Chapman & Hall, New York.

Tellam, R. L., G. Wijffels and P. Willadsen, 1999 Peritrophic matrix proteins. Insect Biochem. Mol. Biol. **29:** 87–101.

Thathy, V., D. W. Severson and B. M. Christensen, 1994 Reinterpretation of the genetics of susceptibility of *Aedes aegypti* to *Plasmodium gallinaceum.* J. Parasitol. **80:** 705–712.

Wang, P., and R. R. Granados, 1997 Molecular cloning and sequencing of a novel invertebrate intestinal mucin cDNA. J. Biol. Chem. **272:** 16663–16669.

Zieler, H., J. P. Nawrocki and M. Shahabuddin, 1999 *Plasmodium gallinaceum* ookinetes adhere specifically to the midgut epithelium of *Aedes aegypti* by interaction with a carbohydrate ligand. J. Exp. Biol. **202:** 485–495.

Communicating editor: Z-B. Zeng